

Risk reduction in reservoir delineation through stochastic property and petrophysical modeling - A Case study: Cambay basin, India.

T.K. Mathuria¹, P.K Jain², Manish Kumar Singh³, Abhishek Moharana³

1. INTEG GEOPIC, ONGC Dehradun. 2. ONGC Vadodara 3. Schlumberger Information Solutions, Vadodara.

Presenting author, Email: tarunnavita@yahoo.com

Abstract:

The present study is an attempt to predict reservoir facies within a sand/shale alternating zone with thin lenticular sand alternations through stochastic modeling of petrophysical, seismic, well data and other geological and geophysical data. G&G data consisting of 3D seismic and well data of number of wells drilled in the study area were integrated with other petrophysical data using petrel software to carry out property modeling of the pay sand which indicated presence of commercial gas and condensate. Various log properties e.g. effective porosity, neutron porosity, permeability, density, water saturation, net-to- gross sand ratio in pay intervals etc at well positions were populated and propagated within the 3D grid volume. Structural framework was generated after converting time grid to depth grid using interval velocity model. Discrete facies and other petrophysical properties were then propagated throughout the 3D grid by horizontal and vertical variogram analysis and application of Sequential Indicator Simulation (SIS), the pixel based algorithm.

Discrete sand/shale facies maps were prepared using different cut off value of log parameter viz. GR, density, and porosity validated by facies logs which were generated using neural network. Seismic inversion studies were carried out using Hampson- Russel software and the results were imported in Petrel 3D grid.

Above analysis resulted in generation of sand distribution maps in the area which is part of regional geological set up, deposited under varying deltaic environments. Distributary channel system has been envisaged from above analysis. Wells drilled in different places in the study area have validated this depositional pattern, and also demonstrated the effectiveness of the geo-statistical modeling.

The integrated seismic to modeling approach adopted in this case study has resulted in precise mapping of the reservoir sand geometries. Higher vertical resolution and accurate layer-by-layer lateral extrapolations of the petrophysical and facies properties effectively improved the stratigraphic interpretation, sedimentary architecture, and lithology prediction which were subsequently used to refine the drilling plan of new exploratory and development wells.

Introduction:

The study area (Fig.1) lies in the Jambusar-Broach sub-block of Cambay Basin and forms a part of north-eastern rising flank of Broach depression. The area is bounded on the north by the river Mahi and Jambusar field in the south. The objective of the study is to know the sand dispersal pattern of Hazad pay sand in well F which produced gas and condensate. The log and testing data of 11 wells drilled in the area reveal that the Hazad sands are lenticular in nature. To know the dispersal pattern of pay sand, stochastic property modelling has been attempted. Different logs properties like effective porosity, NPHI porosity, permeability, density, effective sand thickness etc. were analyzed through property modeling and were propagated within the 3D depth grid by horizontal and vertical variogram analysis and applying Sequential Indicator Simulation (SIS) pixel based algorithm resampled by Acoustic Impedance as secondary property in Schlumberger Petrel software. Discrete sand shale facies maps were generated by giving different cutoff in GR, Density and Porosity logs which are validated by Facies generated by neural network. The seismic inversion studies were carried out using Hampson-

Russel software and then were imported in Petrel 3D grid. The integrated facies, petrophysical modeling and inversion studies suggest that there are three distributary channel lobes separated by interdistributary shale. The main sand lobe is having a thickness of 4m in SW-NE direction encompassing wells, D, E, and F. Second lobe is developed around wells G and H, separated from main channel by inter-distributary shales. Third sand lobe is developed around wells A, B and C in the northeastern part of the study area. The pay zone is confined to first lobe near well F. This approach is applied in a geostatistical workflow to better integrate available geologic information. The resulting models may improve the accuracy of model reservoir response and account for the uncertainty in the heterogeneity of deltaic lobes.

Geological setting:

The study area (Fig.1) lies in the Jambusar-Broach sub-block. In the basinal part, tertiary and quaternary sedimentary sequence of over 5000m thickness unconformably overlies Deccan Trap. In the early phase of sedimentation, Trap wash/ conglomerate/clay stone facies of Olpad Formation were deposited under fluvial environment. After this, widespread marine transgression covered the basin and thick Cambay Shale was deposited during Upper Paleocene to Early Eocene period. This was followed by various regressive and transgressive cycles. The sandy facies of Hazad, Ardol, Dadhar, Tarkeshwar, and Babaguru were deposited during various regressive phases. These regressive phases were interrupted by minor transgressive cycles giving rise to the deposition of shaly facies of Kanwa, Telwa and intervening shales of Tarkeshwar and Babaguru formations. The Hazad sands are the major hydrocarbon producers in the basin (Fig.2). The study area form the part of Upper delta plain and deposits are inter distributaries channels separated by inter distributary shale. The log and testing data of 9 wells drilled in the block reveal that the Hazad sands are lenticular in nature. The sands occur as isolated lobes and the orientation of these lobes are highly influenced by Tidal actions.

Methodology:

The study was under taken in Petrel software to bring out the depositional model of GS-6 pay sand by integrating property modeling of facies and petrophysical properties with seismic attributes. The workflow shows the main input is seismic grid. Different logs and facies properties were upscaled and populated within the depth grid by geostatistical algorithm for reservoir delineation (Fig.3).

Structural Modeling:

- **Horizon/Well Marker Interpretation:** Initially Horizon mapping of 8 seismic markers corresponding to Trap top, OCS top, Y-Marker, GS-6 sand, Hazad top, Dadhar top and high amplitude event within Dadhar formation was carried out in the area. However for present study only five formation tops namely, Hazad top, GS-6 sand top, Y-Marker, OCS top and Olpad top were mapped and four reservoir zones were created between them.
- **Structural Framework:** The 3D Skeleton time grids were constructed incorporating the fault framework by Corner point gridding process and top, middle and base structural framework were prepared (Fig.5, 6&7). The horizon surfaces were then integrated in the 3D Structural framework time grid.
- **Zones and Layering:** The study was focused to know the extension of GS-6 pay sand. Four Zones are prepared i.e. Zone-1 (Hazad top to GS-6 top), Zone-2 (GS-top to Hazad bottom), Zone-3 (Y-Marker to OCS top) and Zone-4 (OCS top to Olpad top). The 100m thick Zone 2 was further subdivided into 50 layers constituting a layer thickness of 2m allowing for fine facies demarcation. Two layers were prepared i.e. Layer-1 (GS-6 top to Hazad bottom) and Layer -II (Hazad Bottom to Y marker). The study was mainly confined to Zone-II, where all the Facies and petrophysical properties were populated along Zone -II (Fig.8).
- **Structure Grid:** Time grids were prepared for all the Horizons incorporating structure fault framework (Fig.9). The velocity model was prepared using PSTM velocities (Fig.10) and time grid was converted to Depth grid by interval velocity model. All the property modeling population was done on depth volume (Fig.11).

Property Modeling:

- **Facies Modeling:** The discrete facies property model was prepared for Zone-II. Sandy, Shaly and Silty Facies were demarcated by GR and Porosity-Density logs and were validated by Facies model using neural network. Different properties were upscaled and were populated along the depth grid by horizontal and vertical variogram analysis and applying Sequential Indicator Simulation (SIS) pixel based algorithm (Fig.3). Different realizations of facies model were analyzed (Fig.4).
- **Petrophysical Modeling:** The continuous petrophysical properties i.e. effective porosity, neutron porosity, log impedance, water saturation and sand net to gross thickness were calculated and populated along the grid by applying Sequential Gaussian Simulation(SGS) algorithm stochastic method (Fig.12&13).

Results and discussion:

The integrated Facies and petrophysical modeling with population of inversion studies in the 3D grid have been very helpful in deciphering the sand distribution pattern. The sand isolith maps were prepared from the actual sand thickness at wells are well matched with property maps. It suggests that there are three distributary channel lobes separated by interdistributary shales. The main sand lobe is having a thickness of 4m in SW-NE direction encompassing wells D, E, and F. Second lobe is developed around wells G and H, separated from main channel by inter-distributary shales. Third sand lobe is developed around wells A, B and C in the northeastern part of the study area (Fig.14). Finally the GIIP map generated shows extension of the pay zone is confined to first lobe near well F (Fig.15).

Conclusions:

The following conclusions could be drawn from this case study:

1. The integrated approach to interpretation adopted in this case study has resulted in precise mapping of the reservoir sand geometries. Higher vertical resolution and accurate layer-by-layer lateral extrapolations of the petrophysical and facies properties population improved the stratigraphic interpretation, sedimentary architecture, and lithology prediction which were subsequently used to refine the drilling plan of new exploratory and development wells.

For this specific reservoir, direct well-seismic calibration does not give satisfactory results because the different seismic attributes values alone are not able to directly separate different lithofacies such as sands and shales.

2. Supported by the above observation, a new workflow was generated to integrate well and seismic data, each with different resolution, into a geologically consistent model. Different petrophysical and facies maps were generated and populated in to 3D grid. Different logs properties like effective porosity, NPHI porosity, permeability, density, effective sand thickness etc. were analyzed though property modeling and were propagated within the 3D grid-volume in the depth domain by horizontal and vertical variogram analysis and applying Sequential Indicator Simulation (SIS) pixel based algorithm. The horizontal variogram is resampled with Acoustic Impedance to interpolate various properties between the wells. The resulting model shows the reservoir extension in the sand lobe of 4m in SW-NE direction encompassing wells D, E, and F (Fig.14). The integrated modeling of lithofacies and petrophysical properties by geostatistical method shows the effectiveness of geostatistical modeling. It gives the sand distribution pattern on the basis of facies and petrophysical properties throughout the 3D depth grid. This is very helpful when there are few wells and constrains seismic attributes.

References:

1. Michael J. P, O Catuneanu, C. V. Deutsch (February 2005); Stochastic surface-based modeling of turbidites lobes AAPG Bulletin, v. 89, no. 2, pp. 177–191.
2. Yuhong. L, A Harding, W. Abriel, and S. Strebelle; (July 2004) Multiple-point simulation integrating wells, three-dimensional seismic data, and geology; AAPG Bulletin, v. 88, no. 7, pp. 905–921.
3. Haldorsen, H., E. Damsleth, 1990, stochastic modeling: Journal of Petroleum Technology, p. 404–
4. D. W. S. Kendall, and J. Mecke, 1987, Stochastic geometry and its applications: New York, John Wiley & Sons, P. 345.
5. Deutsch, C. V., 2002, Geostatistical reservoir modeling: New York, Oxford University Press, 376 p.

6. Methodology for Integrating Analog Geologic Data in 3-D Variogram Modeling AAPG Bulletin, V. 83, No 8. P. 1262–1278 A.
7. Bose, V. Singh, A.K. Tandon, B.S. Josylu, and M. Chandra October 2004; Case study of stratigraphic and lithology interpretation of thin reservoirs through an integrated approach, The Leading Edge.
8. Orellana N, Cavero J: Influence if variograms in 3D reservoir modeling outcomes: an example. The Leading Edge August 2014 P 890-902.
9. Best practice stochastic facies modeling for the channel fill turbidite sandstone analog (the Quarry outcrop Eocene Ainsa basin, northeast Spain) AAPG Bulletin, v 90, no. 7, pp. 1003 –1029.

Acknowledgments:

Authors are grateful to management of ONGC Ltd for according permission to contribute this paper.

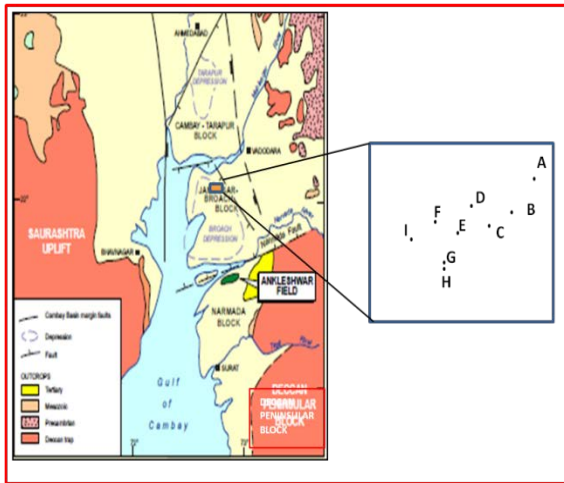


Figure 1. Map of Cambay Basin India, showing the study area and wells drilled .

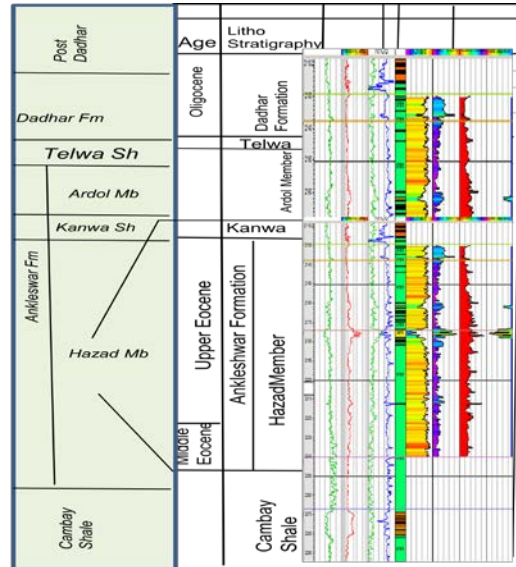


Figure 2. Generalized stratigraphy of study area.

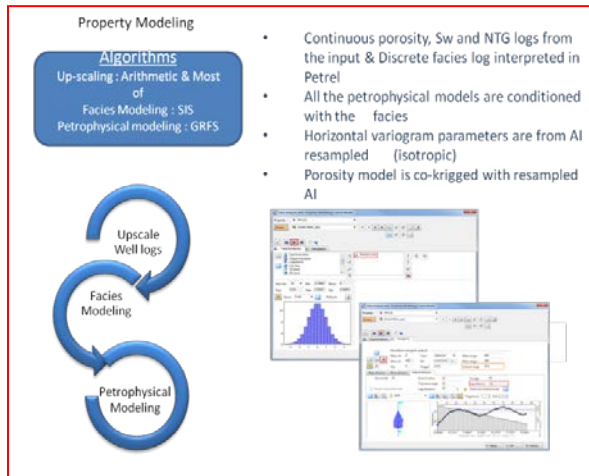


Figure 3. Property Modelling Workflow.

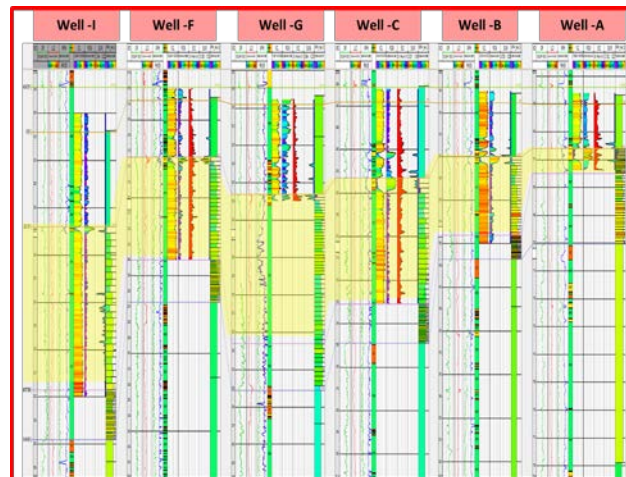


Figure 4. Petrophysical Analysis Through Wells A-F showing Facies Definition and Upscaled logs.

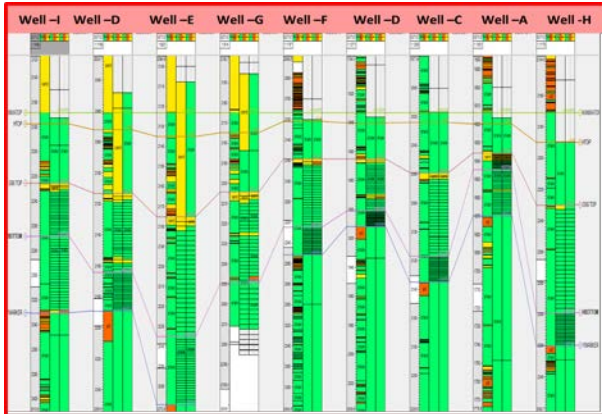


Figure 4. Facies analysis derived from logs value cut off and Neural Network.

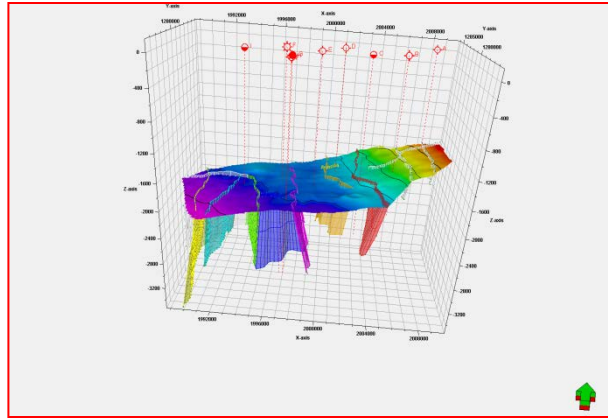


Figure 5. Structural framework derived from Fault Polygons

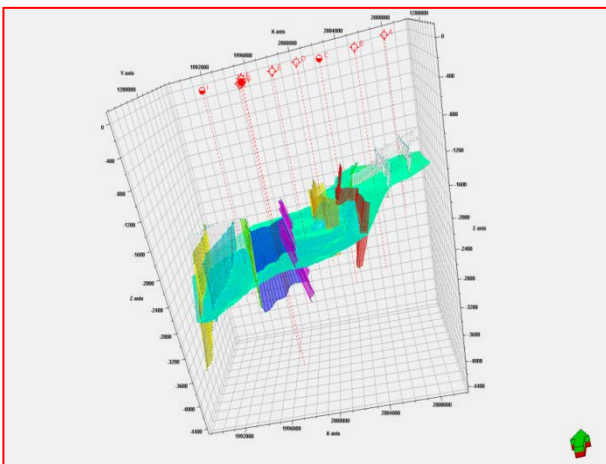


Figure 6. Fault framework with GS-6 pay horizon.

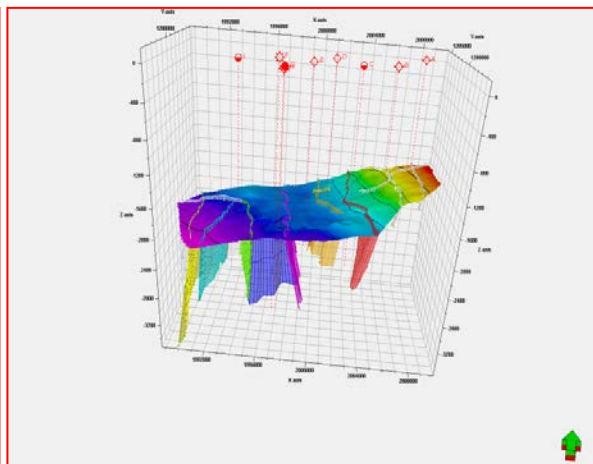


Figure 7. Time grid of GS-6 pay sand having zones and layers point pillar gridding.

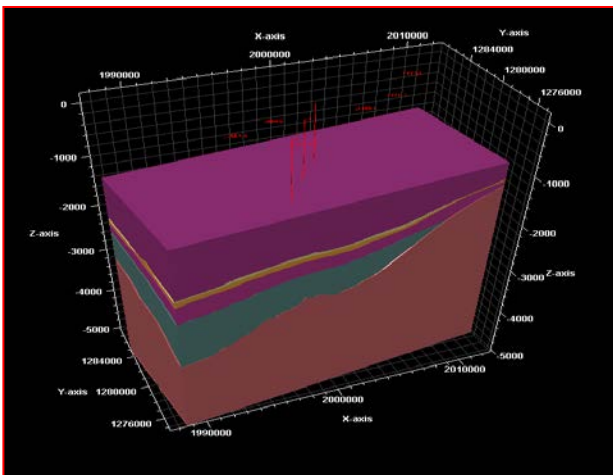


Figure 8. Structural Framework showing zones and layers.

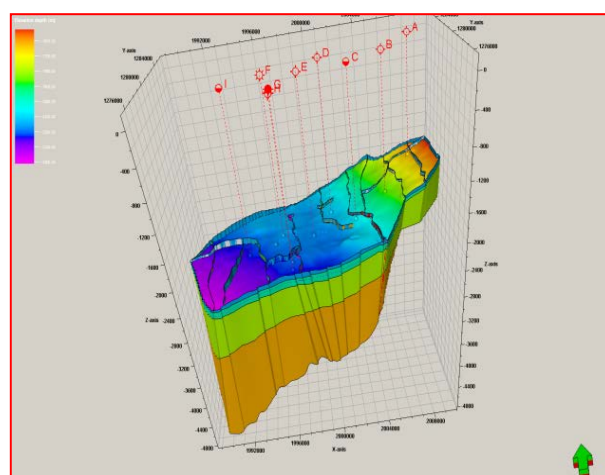


Figure 9. Time grid of GS-6 pay sand having zones and layers with well tops.

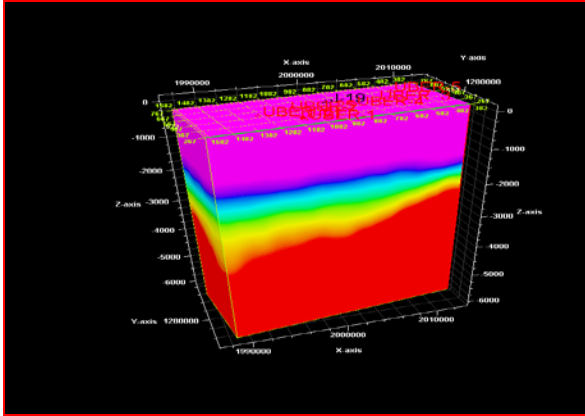


Figure 10. Interval velocity cube used for domain conversion.

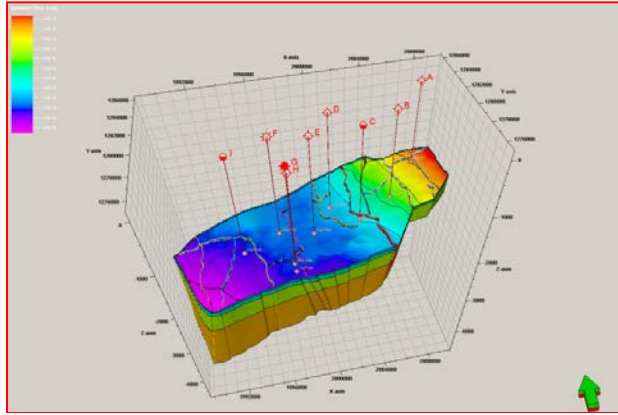


Figure 11. Depth Map of Hazad pay sand derived from domain conversion.

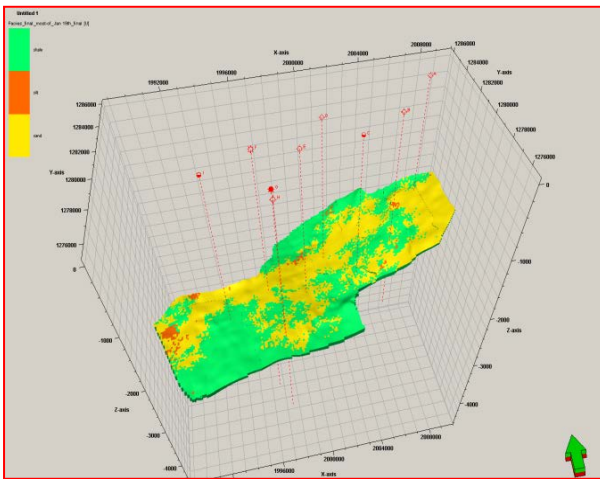


Figure 12. Facies Map showing sand and shale distribution.

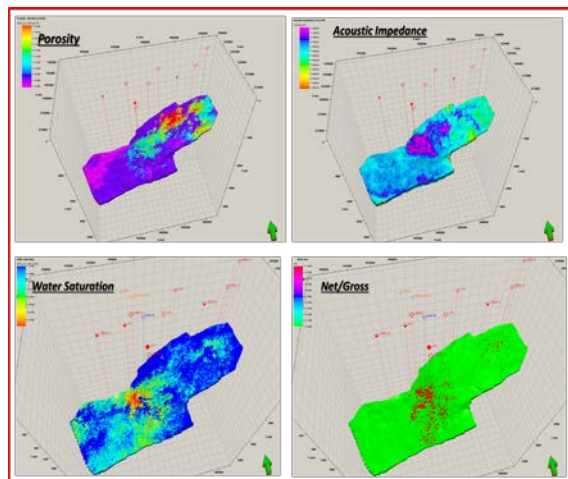


Figure 13. Depth grid showing petrophysical properties & acoustic impedance



Figure 14. Sand Isolith Map derived from Property modelling.

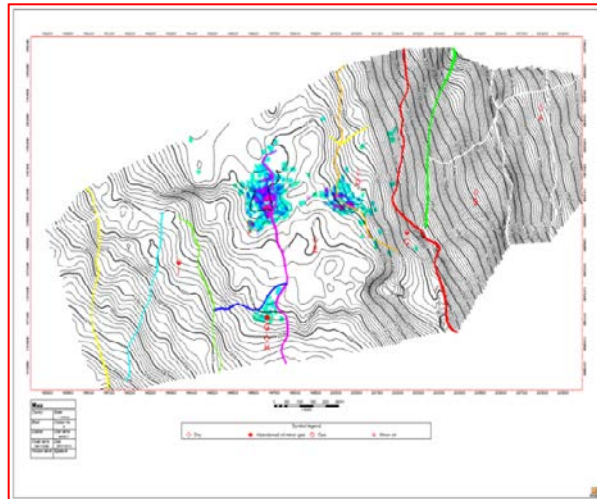


Figure 15. GIP Map derived from Property modelling.